Philosophical Magazine

ISSN: 1478-6435 (Print) 1478-6443 (Online) Journal homepage: https://www.tandfonline.com/loi/tphm20

High-pressure torsion-induced grain growth and detwinning in cryomilled Cu powders

Haiming Wen , Yonghao Zhao , Ying Li , Osman Ertorer , Konstantin M. Nesterov , Rinat K. Islamgaliev , Ruslan Z. Valiev & Enrique J. Lavernia

To cite this article: Haiming Wen , Yonghao Zhao , Ying Li , Osman Ertorer , Konstantin M. Nesterov , Rinat K. Islamgaliev , Ruslan Z. Valiev & Enrique J. Lavernia (2010) High-pressure torsion-induced grain growth and detwinning in cryomilled Cu powders, Philosophical Magazine, 90:34, 4541-4550, DOI: 10.1080/14786435.2010.514579

To link to this article: https://doi.org/10.1080/14786435.2010.514579

Philosophical Magazine
Vol. 90, No. 34, 28 November 2010, 4541–4550

Taylor & Francis
Taylor & Francis Group

High-pressure torsion-induced grain growth and detwinning in cryomilled Cu powders

Haiming Wen[a], Yonghao Zhao[a], Ying Li[a], Osman Ertorer[a], Konstantin M. Nesterov[b], Rinat K. Islamgaliev[b], Ruslan Z. Valiev[b] and Enrique J. Lavernia[a]*

[a]*Department of Chemical Engineering and Materials Science, University of California, Davis, CA 95616, USA;* [b]*Institute of Physics of Advanced Materials, Ufa State Aviation Technical University, Ufa 450000, Russia*

(*Received 10 June 2010; final version received 4 August 2010*)

Two mechanisms for deformation-induced grain growth in nanostructured metals have been proposed, including grain rotation-induced grain coalescence and stress-coupled grain boundary (GB) migration. A study is reported in which significant grain growth occurred from an average grain size of 46 nm to 90 nm during high pressure torsion (HPT) of cryomilled nanocrystalline Cu powders. Careful microstructural examination ascertained that grain rotation-induced grain coalescence is mainly responsible for the grain growth during HPT. Furthermore, a grain size dependence of the grain growth mechanisms was uncovered: grain rotation and grain coalescence dominate at nanocrystalline grain sizes, whereas stress-coupled GB migration prevails at ultrafine grain sizes. In addition, detwinning of the preexisting deformation twins was observed during HPT of the cryomilled Cu powders. The mechanism of detwinning for deformation twins was proposed to be similar to that for growth twins.

Keywords: nanocrystalline metal; deformation-induced grain growth; grain rotation; grain coalescence; grain boundary migration; detwinning

1. Introduction

Plastic deformation of coarse-grained metals operates mainly on the basis of the nucleation and motion of lattice dislocations. However, in the case of nanocrystalline (nc) metals, when the grain size decreases below a certain value, the deformation mechanisms involve grain boundary (GB)-mediated processes such as GB sliding, grain rotation, GB migration, and GB diffusion [1–5]. Deformation-induced grain growth in nc metals has been widely reported and it reveals GB-mediated processes during deformation of nc metals. Experimentally, deformation-induced grain growth has been documented in various plastic deformation processes including nanoindentation [6], high pressure torsion [7,8], uniaxial tension [9–11], uniaxial compression [12,13], and *in situ* TEM straining [5,14–16]. Moreover, molecular dynamics (MD) simulations [17–20] and theoretical model analyses [20–22]

*Corresponding author. Email: lavernia@ucdavis.edu

ISSN 1478–6435 print/ISSN 1478–6443 online

DOI: 10.1080/14786435.2010.514579
http://www.informaworld.com

have been carried out in an effort to understand the mechanisms that govern deformation-induced grain growth. In essence, a review of the published literature suggests that two different mechanisms have been proposed, i.e. grain rotation-induced grain coalescence and stress-coupled GB migration. Despite these published studies, the question of which of these two mechanisms is responsible for the grain growth during deformation remains unresolved. Noteworthy, *in situ* TEM investigations revealed contradictory results, in which Shan et al. [5] and Wang et al. [16] observed rotation of grains of 10–20 nm in size, which brought their orientations closer together and finally led to the elimination of GBs and coalescence of nanograins into larger grains; whereas Jin et al. [14] and Legros et al. [15] recorded GB migration from larger grains (>100 nm) toward smaller grains, that is, growth of larger grains at the expense of smaller grains. In view of this lack of fundamental information, the present study was conducted in an effort to provide insight into the mechanism(s) that govern deformation-induced grain growth as well as to establish any grain size dependence.

A significant reduction of twin density (detwinning, i.e. the reverse process of twinning) has been reported during dynamic compression of an electrodeposited nc Ni–Fe alloy, thereby suggesting an additional deformation mechanism in nc metals [13]. The phenomenon of detwinning has also been observed during rolling [23] as well as during *in situ* nanoindentation [24] of sputtered nanotwinned Cu films. In all of these studies, the detwinning phenomena have been documented in the case of growth twins. This observation raises two important questions. First, would detwinning occur under other deformation conditions? Second, could deformation twins be detwinned?

In this work, we applied high pressure torsion (HPT) to deform and consolidate nc Cu powders produced by cryomilling. Significant deformation-induced grain growth was observed, which was attributed to grain rotation and grain coalescence after careful microstructural examination. In addition, detwinning during HPT was identified for the case of preexisting deformation twins in the as-cryomilled Cu powders.

2. Experimental

Cryomilling was used to prepare nc Cu powders. Cryomilling is a mechanical attrition technique in which powders are milled in a cryogenic liquid [25]. Coarse-grained Cu powders were cryomilled for 8 h in liquid nitrogen with a ball to powder ratio of 30:1. HPT was applied to deform and consolidate the cryomilled Cu powders under a pressure of 6 GPa for 20 revolutions at room temperature and a rotational speed of 1 revolution per minute. The experimental arrangement used in the present work is similar to that described in detail elsewhere [26]. It is worth noting that available results suggest that the thermal energy generated in the sample during torsion is quickly conducted away into the massive HPT anvils [7]; this is supported by our experimental measurements which showed that the temperature of the sample during torsion was lower than 40°C. Consolidation of cryomilled powders by HPT produced thin disks with thickness of approximately 1 mm and diameter of 10 mm.

Scanning electron microscopy (SEM) and transmission electron microscopy (TEM) were used to characterize microstructures of as-cryomilled Cu powders and bulk Cu sample processed by HPT (hereafter referred to as HPT Cu sample). SEM imaging was performed by a FEI XL30-SFEG microscope using a voltage of 15 kV. TEM observations were carried out on a Philips CM12 microscope working at 120 kV and a JEOL 2500SE microscope operating at 200 kV. The procedures for preparing TEM samples are described as follows. For as-cryomilled Cu powders, epoxy was used to glue powders together into a bulk sample and thin foils were obtained by grinding the bulk sample. In the case of the HPT Cu sample, thin foils were sectioned from near the edges of the HPT disk. The TEM specimens were obtained by mechanically grinding and dimpling the thin foils to a thickness of ~10 μm, and further thinning to electron transparency using a Gatan PIPS 691 ion milling system.

3. Results and discussion

Cryomilling for 8 h generated irregularly shaped Cu particles/agglomerates with a size of approximately 50 μm, as shown in the SEM image (Figure 1a) of the cryomilled Cu powders. Cryomilling usually results in micron-sized powder

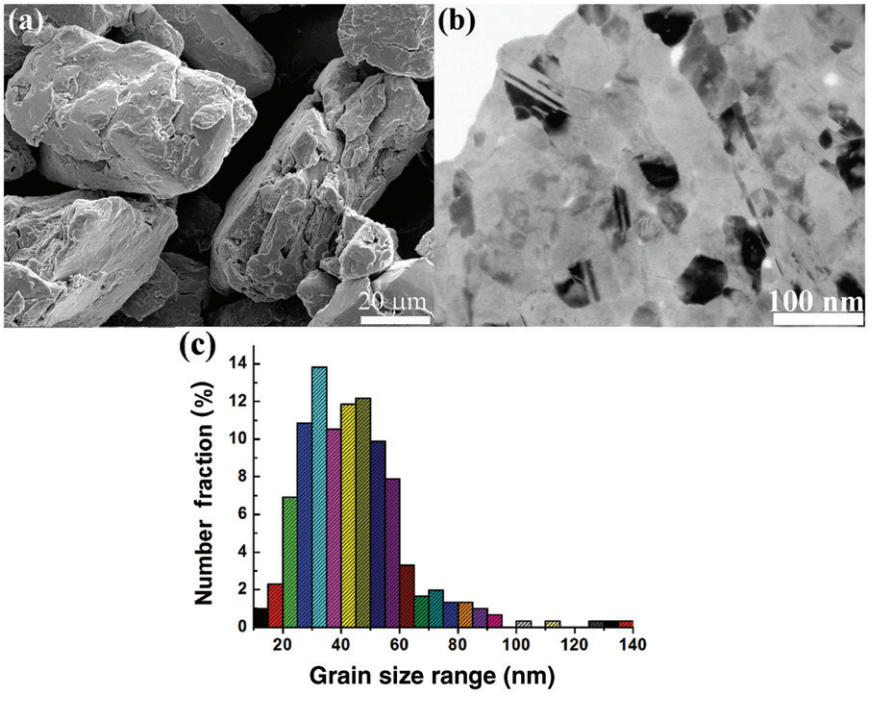

Figure 1. Microstructural characteristics of the as-cryomilled Cu powders: (a) SEM image showing micron-sized powder particles/agglomerates; (b) TEM image showing equiaxed nanograins with fraction of twinned grains of 20%; (c) statistical grain size distribution from ~400 grains, with average grain size of 46 nm.

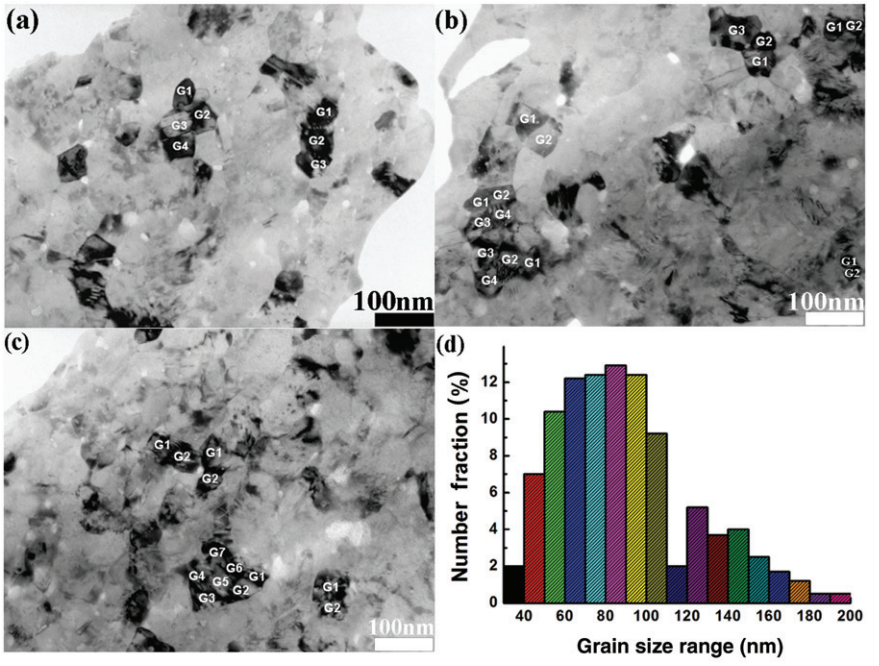

Figure 2. (a–c) TEM images and (d) statistical grain size distribution of the HPT Cu sample. The average grain size is 90 nm, indicating significant grain growth during HPT. Large grains are composed of several subgrains, which are labeled as G1, G2, G3, etc. The fraction of twinned grains was significantly reduced to 9%.

particles/agglomerates because of significant cold welding during milling [27]. Large-area TEM observations indicated that the cryomilling process produced randomly-distributed equiaxed nanograins as representatively shown in Figure 1b with a bright-field TEM image. The contrast between adjacent grains is high. Statistical grain size analysis from about 400 grains shows that the grain size distribution is narrow with most grains in the range of 20–60 nm (Figure 1c). The average grain size is 46 nm. Aspect ratios of grains were also analyzed during the grain size analysis and the mean aspect ratio was determined to be 1.34, which is consistent with the equiaxed morphology of the grains in the TEM images. In addition, nano-scale deformation twins were frequently observed in some grains, and statistics indicated that the fraction of twinned grains (the ratio of the number of twinned grains to the total number of grains counted) was 20%.

Following the HPT process, significant grain growth was observed, as revealed by the TEM images (Figures 2a–c) and the grain size distribution (Figure 2d). It can be seen that grains are much larger than those in the as-cryomilled powders. From the statistical grain size analysis, the average grain size of the HPT sample is 90 nm, i.e. nearly twice that of the as-cryomilled powders (46 nm). More careful TEM inspection revealed that most large grains in the HPT sample are composed of several subgrains, which are labeled as G1, G2, G3, etc., in the TEM images. This can be easily seen when a large grain is on or close to a major zone axis so that the

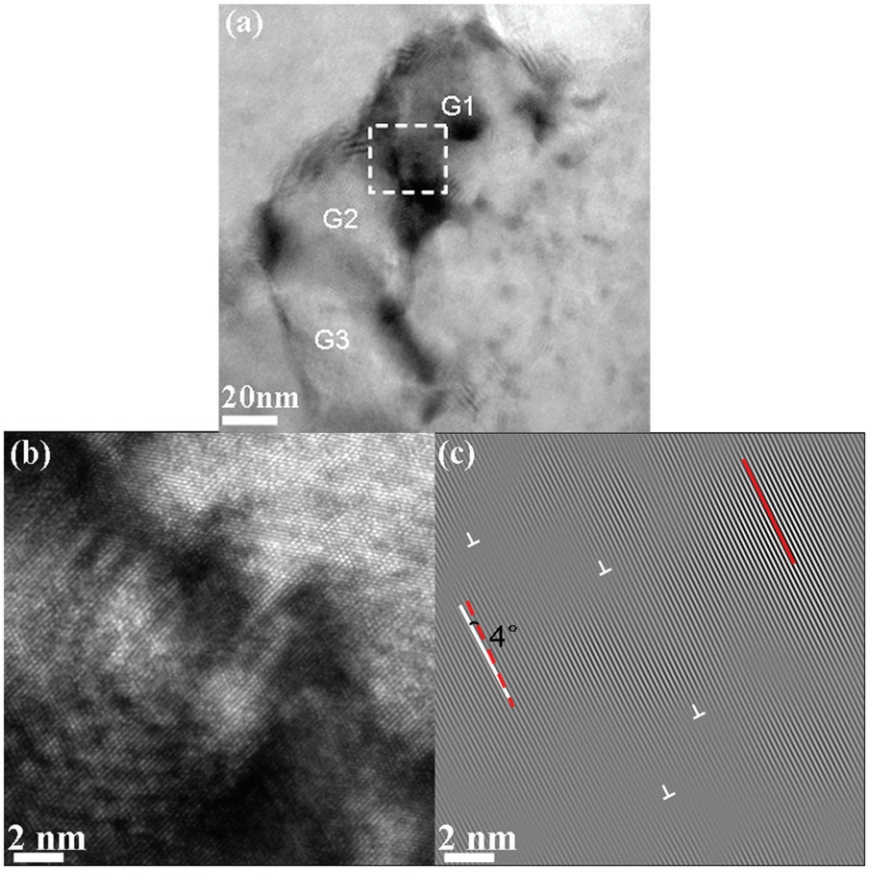

Figure 3. (a) TEM image of a large grain in the HPT Cu sample, which is composed of three small subgrains (G1, G2, G3); (b) a magnified view of the white rectangle area in (a) showing the subgrain boundary between G1 and G2; (c) the $(\bar{1}1\bar{1})$ planes in G1 and G2 obtained by inverse Fourier transformation of (b), showing a small misorientation angle of 4° between G1 and G2. Dislocations located at the subgrain boundary are marked with white 'T' at the dislocation cores.

grain appears dark in the bright-field TEM image, but within the grain each subgrain has slightly different contrast and the subgrain boundaries can be identified.

In order to confirm that large grains in the HPT Cu sample are composed of several small subgrains, high-resolution TEM (HRTEM) was used to investigate subgrain boundaries within some large grains. Figure 3a shows a grain which is composed of three small subgrains (G1, G2, G3). Figure 3b is a magnified view of the white rectangle area (the boundary between G1 and G2) in Figure 3a and the subgrain boundary can be clearly seen. Figure 3c shows the $(\bar{1}1\bar{1})$ planes in G1 and G2 obtained by inverse Fourier transformation of Figure 3b. The misorientation angle between G1 and G2 can be obtained by drawing two straight lines parallel to the $(\bar{1}1\bar{1})$ planes in G1 and G2, respectively, and measuring the angle between the

two lines. The misorientation angle was measured to be 4°, indicating a small-angle subgrain boundary. In addition, some dislocations, marked with white 'T' at the dislocation cores, are aligned at the subgrain boundary.

The TEM analyses above indicate that large grains in the HPT Cu sample were formed during HPT through rotation and coalescence of the initial small grains in the cryomilled Cu powders. Although our study is through postmortem microstructure analysis, *in situ* TEM investigations [5,16] have revealed the real-time processes of grain rotation and grain coalescence. Moreover, some models have been developed for this mechanism [16,22]. With plastic deformation, grain boundary sliding occurs via gliding GB dislocations. A gliding GB dislocation splits at triple junction into two climbing GB dislocations, and the crystal lattice rotation in the neighboring grain will subsequently occur by these climbing GB dislocations (GB sliding transforms into rotation of neighboring grain). Successive multiple rotations of neighboring grains bring their orientations closer together and this leads to the decrease of GB misorientation angles and even elimination of GBs, which finally causes coalescence of nanograins into larger grains. This is also consistent with observations of MD simulations [17,28]. Coalescence of grains reduces the total GB energy in the system.

Except for the large grains containing several subgrains, some small equiaxed grains with size and morphology similar to those of the grains in the cryomilled powders were also observed in the HPT sample. This observation indicated that not all initial nanograins coalesced into large grains during HPT. The grain size distribution in Figure 2d further confirms this suggestion, in which a low percent of grains with sizes of 30–50 nm is documented. Moreover, a minority of large grains in the HPT sample was found to be devoid of subgrain structure, implying that GBs had been eliminated and grain coalescence was complete. These results indicate that the processes of grain rotation and grain coalescence are not homogeneous.

In order to ascertain if GB migration played a role in the grain growth during HPT, statistical grain/subgrain size/morphology analyses were carried out in the HPT sample on the subgrains which have coalesced as well as on grains which have not rotated together. The grain/subgrain size distribution is shown in Figure 4, and it is similar to the grain size distribution corresponding to the cryomilled Cu powders (Figure 1c). The average grain/subgrain size is 48 nm, which is very close to the mean grain size of the cryomilled Cu powders (46 nm). The average aspect ratio of grains is 1.37, which is also virtually identical to that of the cryomilled Cu powders (1.34). These quantitative results indicate that GB migration was negligible during HPT. In addition, the irregularly shaped GBs of the large grains in the HPT sample provide additional support to the suggestion that grain growth resulted from grain coalescence induced by grain rotation, rather than from GB migration.

As discussed previously, *in situ* TEM investigations recorded two different grain growth mechanisms corresponding to two size regimes: rotation and coalescence of grains of 10–20 nm in size in the work by Shan et al. [5] and Wang et al. [16], and grain growth via GB migration for grains larger than 100 nm based on the results by Jin et al. [14] and Legros et al. [15]. These results imply that there is a grain size dependence of the mechanisms of deformation-induced grain growth.

In view of the above discussion, we will first establish the influence, if any, of grain size on grain rotation-induced grain coalescence. The model developed by

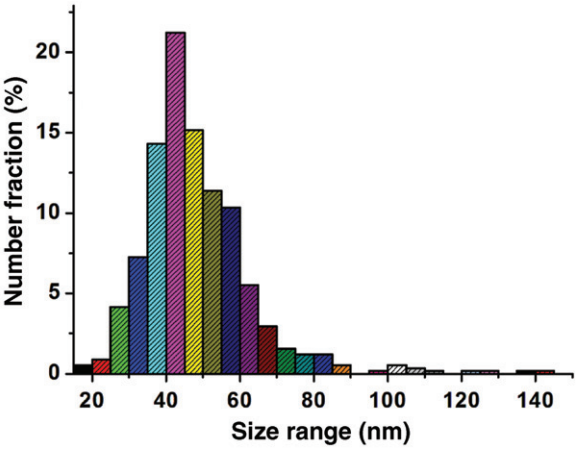

Figure 4. Statistical grain/subgrain size distribution of the subgrains which have coalesced and grains which have not rotated together in the HPT Cu sample. The average grain/subgrain size is 48 nm, which is almost the same as the mean grain size of the cryomilled Cu powders (46 nm), indicating that the grain growth during HPT resulted from grain coalescence induced by grain rotation, rather than GB migration.

Moldovan et al. [21] was used to rationalize the experimental results of Shan et al. [5]. Grain rotation would create along the periphery of the grain some volumes where grains overlap and leave behind voids in other regions. Such voids and overlapping regions can be avoided by diffusion from the overlapping regions into the voids. The model assumes that grain rotation is accommodated by diffusion, especially GB diffusion in the case of nc materials with very small grain sizes. This assumption should be valid even at room temperature since, for nanograins, GB diffusion at room temperature can be much more significant than that for conventional micrograins, because of the much higher fraction of grain boundaries and the much shorter diffusion pathways. The model ultimately yields a d^{-4} dependence of the grain rotation rate, where d is the grain size. Therefore, grain rotation rate has a marked dependence on grain size. For nc metals with a grain size much smaller than 100 nm, grain rotation rate, and grain coalescence accordingly, are very significant. As grain size is increased above a certain value (e.g. 100 nm), grain rotation and grain coalescence become insignificant and GB migration may take their place. The mechanism of stress-coupled GB migration is based on the argument that shear stress causes tangential movement of grains along GBs (GB sliding), and this produces a coupling with the normal motion of GBs (GB migration) [15,19,20]. The competition between grain rotation and GB migration lies in whether GB sliding transforms into grain rotation or couples with GB migration. From the results of *in situ* TEM investigations by Shan et al. [5] and Wang et al. [16], and Jin et al. [14] and Legros et al. [15], grain rotation outweighs GB migration when grain size is below a certain value, and vice versa. Careful consideration of the two mechanisms of deformation-induced grain growth leads to possible explanation of the contradictory experimental results that are reported in the literature. For the materials used

in the present study with a grain size of ~40 nm, grain rotation and grain coalescence dominate GB migration and hence are the mechanism responsible for deformation-induced grain growth. However, this does not imply that the two mechanisms have to be mutually exclusive or that only one of them can be solely responsible for grain growth. It can be expected that for some grain sizes (especially those around 100 nm) and under some specific conditions, both mechanisms can be active.

In addition to grain growth, another important phenomenon observed during HPT was a significant reduction in the fraction of twinned grains, which is typically described as 'detwinning'. Statistical analysis indicated that the fraction of twinned grains was reduced from 20% in the as-cryomilled powders to 9% in the HPT sample. In order to understand the detwinning process during HPT, HRTEM was applied to investigate some twin boundaries in the HPT sample. Figure 5a shows

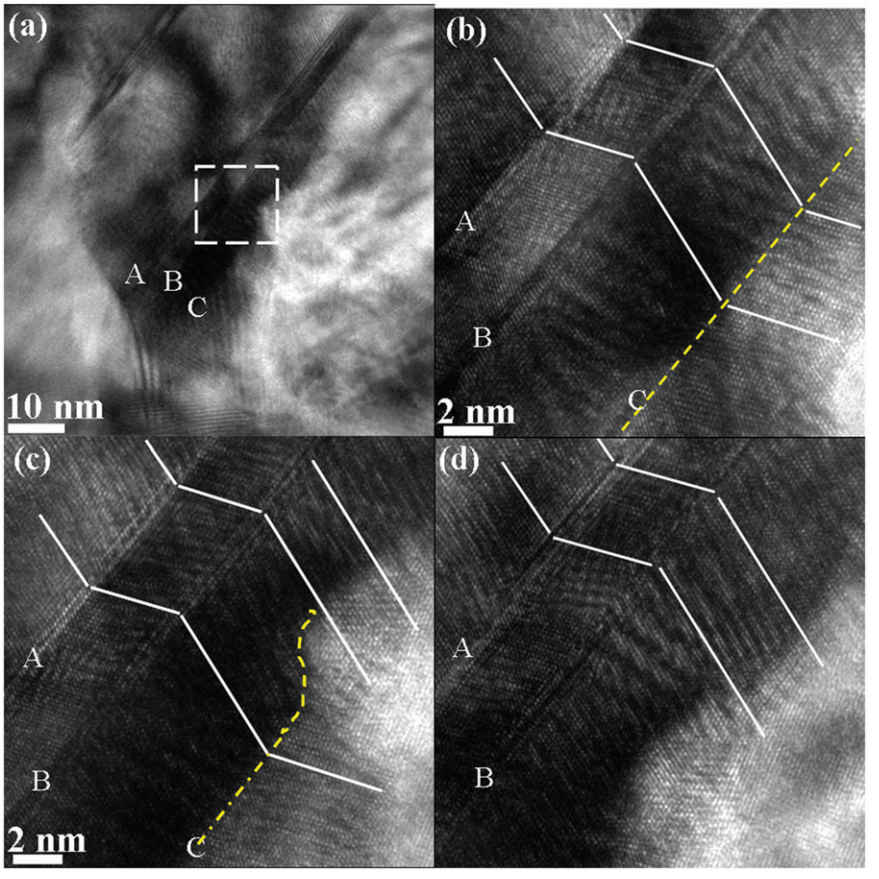

Figure 5. Some twin boundaries in the HPT Cu sample. (a) TEM image showing three twin boundaries in a grain which are labeled A, B, C. The white rectangular area in (a) was magnified, and (b–d) were taken successively along the three twin boundaries from lower left to upper right. Twin boundaries A and B are straight and run all the way through the grain. Twin boundary C is initially straight, but then becomes distorted and finally is eliminated.

three twin boundaries, which are labeled A, B, C in a grain. The white rectangular area in Figure 5a was magnified, and the images in Figures 5b–d were taken successively along the three twin boundaries from lower left to upper right. It can be seen that twin boundaries A and B are straight and run all the way through the grain. However, twin boundary C is initially straight, but then it becomes distorted and finally it is eliminated. This is very similar to what was observed using *in situ* TEM during nanoindentation of sputtered nanotwinned Cu films in which the detwinning process of growth twins was recorded [24]. The distorted part of twin boundary C probably contains steps with a height of multiple atomic planes. Using topological analysis and MD simulations, mechanisms of detwinning were elucidated in [24]. For twins in fcc lattices, either deformation or growth twins, their ends can be represented as incoherent twin boundaries (ITBs) formed by an array of Shockley partial dislocations [29,30]. A detwinning process is accomplished via migration of ITBs, and ITBs migrate through the collective glide of multiple twinning dislocations that form the ITBs. ITBs propagate as disconnections or steps with a height of multiple atomic planes. Therefore, the detwinning process occurs by migration of steps or disconnections with step heights of the order of a few interplanar distances. This was also observed in the case of detwinning of growth twins in an electrodeposited nc Ni–Fe alloy during dynamic compression [13]. The work reported in this paper reveals that detwinning can happen during HPT and it should be a generic process during deformation of nc metals with either growth twins or deformation twins. Moreover, the detwinning mechanism for deformation twins is probably very similar to that for growth twins. As reported in [13], detwinning serves as another deformation mechanism and can significantly influence mechanical behavior of nc metals.

4. Conclusions

In summary, significant grain growth was observed during high pressure torsion of nanocrystalline Cu powders with an average grain size of 46 nm prepared by cryomilling. The mechanism of the grain growth was determined to be grain rotation-induced grain coalescence. By carefully considering the two mechanisms of deformation-induced grain growth, grain size dependence of the mechanisms was uncovered. For nanograins with size much smaller than 100 nm, grain rotation-induced grain coalescence is the dominant mechanism of grain growth; while grain growth should be primarily attributed to stress-coupled grain boundary migration when grain size is larger than 100 nm. Detwinning of the preexisting deformation twins was revealed during high pressure torsion of the cryomilled Cu powders. The mechanism of detwinning for deformation twins is probably very similar to that for growth twins, which involves the collective glide of multiple twinning dislocations.

Acknowledgement

The authors would like to acknowledge financial support by the Office of Naval Research (Grant No. ONR N00014-08-1-0405).

References

[1] H. Van Swygenhoven and P.M. Derlet, Phys. Rev. B 64 (2001) p.224105.
[2] H. Van Swygenhoven, Science 296 (2002) p.66.
[3] J. Schiøtz and K.W. Jacobsen, Science 301 (2003) p.1357.
[4] V. Yamakov, D. Wolf, S.R. Phillpot, A.K. Mukherjee and H. Gleiter, Nat. Mater. 3 (2004) p.43.
[5] Z.W. Shan, E.A. Stach, J.M.K. Wiezorek, J.A. Knapp, D.M. Follstaedt and S.X. Mao, Science 305 (2004) p.654.
[6] K. Zhang, J.R. Weertman and J.A. Eastman, Appl. Phys. Lett. 87 (2005) p.061921.
[7] X.Z. Liao, A.R. Kilmanetov, R.Z. Valiev, H.S. Gao, X.D. Li, A.K. Mukherjee, J.F. Bingert and Y.T. Zhu, Appl. Phys. Lett. 88 (2006) p.021909.
[8] Y.B. Wang, J.C. Ho, X.Z. Liao, H.Q. Li, S.P. Ringer and Y.T. Zhu, Appl. Phys. Lett. 94 (2009) p.011908.
[9] G.J. Fan, L.F. Fu, H. Choo, P.K. Liaw and N.D. Browning, Acta Mater. 54 (2006) p.4781.
[10] D.S. Gianola, S. Van Petegem, M. Legros, S. Brandstetter, H. Van Swygenhoven and K.J. Hemker, Acta Mater. 54 (2006) p.2253.
[11] T.J. Rupert, D.S. Gianola, Y. Gan and K.J. Hemker, Science 326 (2009) p.1686.
[12] G.J. Fan, Y.D. Wang, L.F. Fu, H. Choo, P.K. Liaw, Y. Ren and N.D. Browning, Appl. Phys. Lett. 88 (2006) p.171914.
[13] S. Cheng, Y.H. Zhao, Y. Guo, Y. Li, Q. Wei, X.L. Wang, Y. Ren, P.K. Liaw, H. Choo and E.J. Lavernia, Adv. Mater. 21 (2009) p.5001.
[14] M. Jin, A.M. Minor, E.A. Stach and J.W. Morris Jr., Acta Mater. 52 (2004) p.5381.
[15] M. Legros, D.S. Gianola and K.J. Hemker, Acta Mater. 56 (2008) p.3380.
[16] Y.B. Wang, B.Q. Li, M.L. Sui and S.X. Mao, Appl. Phys. Lett. 92 (2008) p.011903.
[17] A.J. Haslam, S.R. Phillot, D. Wolf, D. Moldovan and H. Gleiter, Mater. Sci. Eng. A 318 (2001) p.293.
[18] J. Schiøtz, Mater. Sci. Eng. A 375–377 (2004) p.975.
[19] F. Sansoz and V. Dupont, Appl. Phys. Lett. 89 (2006) p.111901.
[20] J. Monk and D. Farkas, Phys. Rev. B 75 (2007) p.045414.
[21] D. Moldovan, D. Wolf and S.R. Phillpot, Acta Mater. 49 (2001) p.3521.
[22] M. Yu. Gutkin, I.A. Ovid'ko and N.V. Skiba, Acta Mater. 51 (2003) p.4059.
[23] O. Anderoglu, A. Misra, J. Wang, R.G. Hoagland, J.P. Hirth and X. Zhang, Int. J. Plast. (2009); DOI: 10.1016/j.ijplas.2009.11.003.
[24] J. Wang, N. Li, O. Anderoglu, X. Zhang, A. Misra, J.Y. Huang and J.P. Hirth, Acta Mater. 58 (2010) p.2262.
[25] D.B. Witkin and E.J. Lavernia, Progr. Mater. Sci. 51 (2006) p.1.
[26] Z. Lee, F. Zhou, R.Z. Valiev, E.J. Lavernia and S.R. Nutt, Scripta Mater. 51 (2004) p.209.
[27] Y. Xun, E.J. Lavernia and F.A. Mohamed, Metall. Mater. Trans. A 35 (2004) p.573.
[28] A.J. Haslam, D. Moldovan, V. Yamakov, D. Wolf, S.R. Phillpot and H. Gleiter, Acta Mater. 51 (2003) p.2097.
[29] J. Wang, O. Anderoglu, J.P. Hirth, A. Misra and X. Zhang, Appl. Phys. Lett. 95 (2009) p.21908.
[30] Q. Hu, L. Li and N.M. Ghoniem, Acta Mater. 57 (2009) p.4866.